

# Cerenkov-like radiation in a binary Schrödinger flow past an obstacle

H. Susanto,<sup>1</sup> P.G. Kevrekidis,<sup>1</sup> R. Carretero-González,<sup>2</sup> B.A. Malomed,<sup>3</sup> D.J. Frantzeskakis,<sup>4</sup> and A.R. Bishop<sup>5</sup>

<sup>1</sup>*Department of Mathematics and Statistics, University of Massachusetts, Amherst MA 01003-4515, USA*

<sup>2</sup>*Nonlinear Dynamical Systems Group, Department of Mathematics and Statistics, and Computational Science Research Center, San Diego State University, San Diego CA, 92182-7720, USA*

<sup>3</sup>*Department of Interdisciplinary Studies, Faculty of Engineering, Tel Aviv University, Tel Aviv 69978, Israel*

<sup>4</sup>*Department of Physics, University of Athens, Panepistimiopolis, Zografos, Athens 15784, Greece*

<sup>5</sup>*Theoretical Division and Center for Nonlinear Studies, Los Alamos National Laboratory, Los Alamos, New Mexico 87545, USA*

We consider the dynamics of two coupled miscible Bose-Einstein condensates, when an obstacle is dragged through them. The existence of two different speeds of sound provides the possibility for three dynamical regimes: when both components are subcritical, we do not observe nucleation of coherent structures; when both components are supercritical they both form dark solitons in one dimension (1D) and vortices or rotating vortex dipoles in two dimensions (2D); in the intermediate regime, we observe the nucleation of a structure in the form of a dark-antidark soliton in 1D; the 2D analog of such a structure, a vortex-lump, is also observed.

*Introduction.* In the past few years, there has been an increasing number of studies of multi-component Hamiltonian systems. This has been triggered primarily by the development of theoretical and experimental results in coupled atomic Bose-Einstein condensates (BECs) [1], and of coupled nonlinear optical systems (where the coupling can be, e.g., between different polarizations of light or different frequencies) [2]. These have, in turn, motivated detailed mathematical investigations of such coupled systems, typically described by nonlinear Schrödinger (NLS) equations [3]. In the setting of BECs, that will be the primary focus of this study, mixtures of different spin states of <sup>87</sup>Rb [4] and <sup>23</sup>Na [5], as well as two-component BECs with different atomic species, such as <sup>41</sup>K-<sup>87</sup>Rb [6] and <sup>7</sup>Li-<sup>133</sup>Cs [7], have been created in experiments. In the same context, a wide variety of theoretical studies have examined ground-state solutions [8] and small-amplitude excitations [9], as well as the formation of other nonlinear structures such as domain walls [10], one-dimensional (1D) bound dark-dark and dark-bright soliton complexes [11], spatially periodic states [12], vortex dipoles [13], vortex rings and slaved waves [14], coupled vortex lattices [15], and so on.

At the same time, many theoretical and experimental studies deal with the dragging of an “impurity” (e.g., a blue-detuned laser beam) through a *one-component* condensate. This setting has been demonstrated to be prototypical for dark soliton formation in 1D [16, 17], and for vortex formation in 2D [18]. These nonlinear waves can be thought of as a type of nonlinear Cerenkov radiation that is emitted, when the motion of the impurity is supercritical with respect to the local speed of sound of the BEC. Recently, a combined experimental and theoretical study of the Cerenkov emission of phonons by a laser obstacle was reported [19]; in a different study [20], it has been shown that in the case of large obstacles (and for a supersonic flow of the BEC), the Cerenkov cone transforms into a spatial shock wave consisting of a chain of dark solitons [20]. In fact, this setting has been particularly relevant for the study of the breakdown of

superfluidity (and emergence of dissipation) and the associated Landau criterion [21]. Indeed, earlier experiments [22] have demonstrated the onset of dissipation, when a blue-detuned laser beam moves through the BEC with velocities above a threshold. We also note in passing that the appearance of similar effects (e.g., the backward-propagating Cerenkov radiation) in photonic crystals [23] is yet another illustration of the interest in this research direction.

In the present work we study the dragging of a  $\delta$ -like obstacle in a *two-component* superfluid flow. If the components are assumed to be immiscible, then they will tend to phase-separate and the problem reverts to its single-component version. For this reason, we consider the case of two miscible components, which is particularly interesting due to the existence of two distinct “speeds of sound”. In this setting, we find two critical speeds  $0 < v_c^{(1)} < v_c^{(2)}$ . For  $v < v_c^{(1)}$ , we show that the impurity propagates without emitting Cerenkov radiation in the form of nonlinear waves. For  $v_c^{(1)} < v_c^{(2)} < v$ , both components are supercritical and the impurity emits gray solitons (in 1D) propagating downstream in both components. However, the most interesting regime is the intermediate one, where one of the components is supercritical, yet the other is subcritical, leading to the spontaneous formation of dark-antidark solitary waves previously predicted (in a stationary form) in [24]. We demonstrate that when the strength of the impurity tends to zero, the critical speeds tend to the corresponding speeds of sound, yet we show how they deviate from these values for finite impurity strengths. We also consider the 2D case, where we also obtain the analog of the dark-antidark state in the form of a vortex-lump wave.

The paper is structured as follows. We first present the theoretical framework, and calculate the critical velocities. We then numerically investigate the 1D (both for untrapped and trapped BECs) and the 2D case. Finally, we summarize our findings and present our conclusions.

*Theoretical Setup.* We consider the following coupled

NLS equations, describing a quasi-1D binary BEC [1]:

$$i\partial_t\psi_j = \left( -\frac{1}{2}\partial_x^2 + \sum_{k=1}^2 g_{jk}|\psi_k|^2 + V_{\text{ext}} \right) \psi_j, \quad (1)$$

where  $\psi_j$  ( $j = 1, 2$ ) are the mean-field wavefunctions, and  $V_{\text{ext}} = V_1 + V_2$  is the external potential, assumed to be composed by a repulsive potential of a blue-detuned laser beam,  $V_1$ , and a trapping harmonic potential,  $V_2$ , i.e.,

$$V_1 = A e^{-(x-vt)^2/2\epsilon^2}, \quad V_2 = \frac{1}{2}\Omega^2 x^2, \quad (2)$$

where  $A$ ,  $\epsilon$  and  $v$  are, respectively, the strength, width and velocity of the laser obstacle, and  $\Omega$  the harmonic trap strength. The nonlinearity coefficients are chosen to be  $g_{11} : g_{12} : g_{22} = 1.5 : 1 : 1.03$ . Notice that two of them have the ratios that are typical for  $^{87}\text{Rb}$  [4], while the third is tuned to a different value (so as to ensure miscibility since the standard value of  $g_{11} = 0.97$  would lead to immiscibility). The tuning can be achieved by means of a Feshbach resonance [25]. Moreover, throughout the paper we use the following parameter values for our numerical computations: chemical potentials  $\mu_1 = 1.2$ ,  $\mu_2 = 1$ , obstacle width  $\epsilon = 0.5$ , and harmonic trap strength  $\Omega = 0.02$ . The results do not change qualitatively for other parameter values.

The uniform solutions of Eqs. (1) satisfy

$$|\psi_1^{(0)}|^2 = \frac{\mu_1 g_{22} - \mu_2 g_{12}}{\Delta}, \quad |\psi_2^{(0)}|^2 = \frac{\mu_2 g_{11} - \mu_1 g_{12}}{\Delta}, \quad (3)$$

where  $\Delta = g_{11}g_{22} - g_{12}^2$ . Expressing Eqs. (1) in the traveling-wave frame (i.e.,  $x \rightarrow x - vt$ ) and linearizing around these uniform states according to  $\psi_j = \psi_j^{(0)} + \psi_j^{(1)}$  we obtain the equations for the small amplitudes  $\psi_j^{(1)}$ ,

$$\frac{1}{4} \frac{d^2}{dx^2} \psi_j^{(1)} = (c_j^2 - v^2) \psi_j^{(1)} + g_{jk} \psi_j^{(0)} \psi_k^{(0)} \psi_k^{(1)}, \quad (4)$$

with  $j, k \in \{1, 2\}$ ,  $k \neq j$  and  $c_j^2 = g_{jj}(\psi_j^{(0)})^2$ . Writing this system as one of four first-order equations (for  $\Psi_j^{(1)} = \dot{\psi}_j^{(1)} \equiv (d/dx)\psi_j^{(1)}$  and  $\psi_j^{(1)}$ ), namely,

$$\begin{pmatrix} \dot{\Psi}_1^{(1)} \\ \dot{\psi}_1^{(1)} \\ \dot{\Psi}_2^{(1)} \\ \dot{\psi}_2^{(1)} \end{pmatrix} = \begin{pmatrix} 0 & c_1^2 - v^2 & 0 & b \\ 1 & 0 & 0 & 0 \\ 0 & b & 0 & c_2^2 - v^2 \\ 0 & 0 & 1 & 0 \end{pmatrix} \begin{pmatrix} \Psi_1^{(1)} \\ \psi_1^{(1)} \\ \Psi_2^{(1)} \\ \psi_2^{(1)} \end{pmatrix}, \quad (5)$$

where  $b = g_{12}\psi_1^{(0)}\psi_2^{(0)}$ . Then, the  $4 \times 4$  matrix has eigenvalues  $\lambda^2 = \tilde{c}^2 - v^2 \pm \sqrt{\tilde{c}^4 - \Delta(\psi_1^{(0)}\psi_2^{(0)})^2}$ , with  $\tilde{c}^2 = (c_1^2 + c_2^2)/2$ . For stability, we need the eigenvalues to be real, hence  $\lambda^2 > 0$  implies that  $v < v_c^{(1)} < v_c^{(2)}$ , where the critical velocities, corresponding to the two distinct speeds of sound, are given by  $v_c^{(1,2)} = \tilde{c} \pm \sqrt{\tilde{c}^4 - \Delta(\psi_1^{(0)}\psi_2^{(0)})^2}$ . For the parameters mentioned above,  $v_c^{(1)} = 0.34393$  and

$v_c^{(2)} = 1.04796$ . We expect that superfluidity will break down when the speed  $v$  of the defect overcomes these speeds; in fact, as argued in [16, 21], the actual critical point should be expected to be lower than the above Landau prediction.

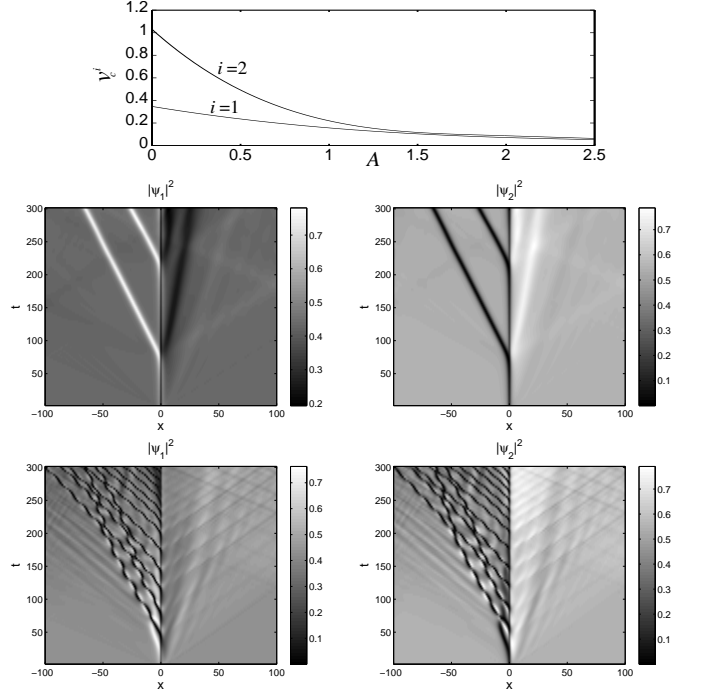


FIG. 1: Top panel: “Stability” boundaries for static dark soliton pairs: the critical velocities for the first and the second component are shown as a function of the impurity strength  $A$ . Middle panels: Space-time evolution of the density contours for the two components in moving coordinate frame with velocity  $v = 0.2$  (the speed of the impurity); clearly the impurity induces the radiation of dark-antidark pairs. Bottom panels: similar to the middle panels but with  $v = 0.3$ , where both dark-antidark dipoles and dark-dark pairs are emitted. Impurity parameters:  $A = 0.9$  and  $\epsilon = 0.5$ .

*Numerical Results.* We now turn to the numerical investigation of the above setting. In Fig. 1, we test the theoretical prediction for the existence of two critical velocities for the dynamical evolution in the two components. The top panel of the figure shows a relevant “bifurcation diagram”, where the dependence of the critical velocities on the “strength”  $A$  of the impurity is numerically evaluated. Note that as the strength of the impurity tends to zero ( $A \rightarrow 0$ ) one recovers the numerical values for  $v_c^{(1,2)}$  stated above. The critical velocities are computed by finding (i) the speed  $v_c^{(1)}$  above which, apparently, one component is supercritical emitting dark solitons, while the other is subcritical emitting antidark solitons (i.e., bright solitons on a finite background) that “accompany” the dark ones; and (ii) the speed  $v_c^{(2)}$  above which both components nucleate dark solitons (see also bottom panel of the figure for a space-time evolution of the density contour plot for the two components for such

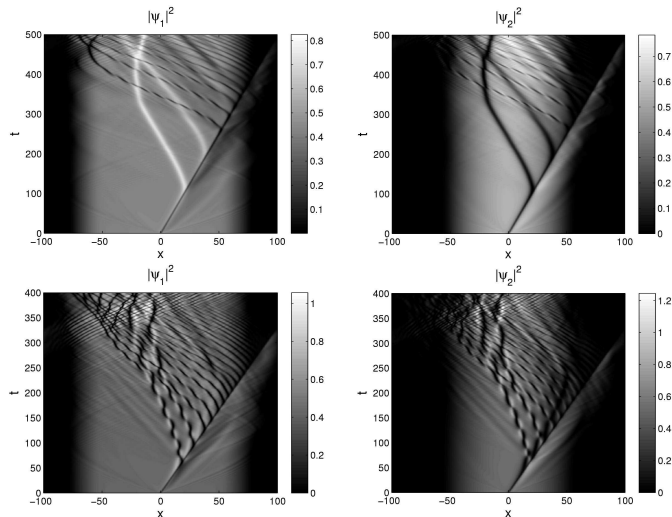


FIG. 2: Space-time contour plots of the components' density, when the obstacle's velocity is  $v = 0.2$  (top panels) and  $v = 0.3$  (bottom panels) in the trapped case ( $\Omega = 0.02$ ). Impurity parameters:  $A = 0.9$  and  $\epsilon = 0.5$ .

a supercritical—in both components—velocity  $v$ ). It is noteworthy that such structures had been predicted in a steady form in [24], but, to our knowledge, this is the first demonstration of their dynamical nucleation. A further observation is worth making about the case of  $v > v_c^{(2)}$ . Note that, especially for early times, the impurity (stationed at  $x = 0$  in the computations of Fig. 1 performed in the co moving frame) initially emits structures that appear more like dark-antidark *dipoles*, i.e., dark-antidark pairs in one-component coupled with antidark-dark pairs in the other component. This is again the first manifestation of such structures (to the best of our knowledge); however, we will make a connection below to their 2D analog that has been previously proposed [26].

The above phenomenology also persists in the presence of an harmonic trap, which is a more realistic setting for magnetically confined BECs. This is clearly shown in Fig. 2, where all parameters are the same as in the corresponding plots of Fig. 1, but incorporating an harmonic trap of frequency  $\Omega = 0.02$ .

We now turn to the 2D case where the second spatial derivatives in Eq. (1) are substituted by the Laplacian and the impurity potential is replaced by its 2D counterpart  $V_1(x, y) = (A/4) \exp(-(x - vt)^2/2\epsilon^2) (\tanh(y + w/2) + 1)(\tanh(-y + w/2) + 1)$ , modeling a light sheet of strength  $A$ , width  $\epsilon$ , and size  $w$  (see elongated vertical bar in panels a and c of Fig. 3). In our 2D simulations we took  $A = 0.9$ ,  $\epsilon = 0.5$  (i.e. same parameters as for the 1D case), and  $w = 10, 15, 20$ . Given the similarities of the trapped and untrapped case in the relevant phenomenology, we only show the latter here. In Fig. 3 we illustrate the two regimes leading to vortex nucleation (the trivial regime for subcritical velocity in both components is not shown here): (A)  $v = 0.235$  is subcritical in the first component, but supercritical in the second, resulting for the latter in a vortex state which is coupled

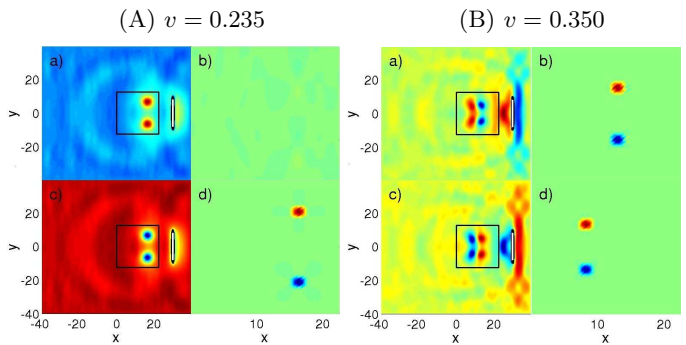


FIG. 3: (Color online). Final snapshots after vortex nucleation for different velocities of a running impurity of size  $w = 10$  (elongated vertical bar in panels a and c). The two depicted cases correspond to: (A)  $v = 0.235$  is subsonic for component  $\psi_1$  and supersonic for component  $\psi_2$ . (B)  $v = 0.350$  is supersonic for *both* components. The top (bottom) panel corresponds to component  $\psi_1$  ( $\psi_2$ ). Left panels (a,c) show the square modulus of the solution together with the moving impurity. The right panels (b,d) show the vorticity  $\omega$  in the rectangular area depicted in the left panel counterparts. Red/blue (top/bottom spots) corresponds to regions with positive/negative vorticity.

to a lump (a 2D structure on a finite background) in the first component. Notice that the presence of vortex states is clearly illustrated in all the figures contained herein, by means of the contours of the vorticity  $\omega = \nabla \times v_s$ , where  $v_s = (\psi^* \nabla \psi - \psi \nabla \psi^*) / i |\psi|^2$  is the velocity field. Such structures have been reported previously for  $g_{11} = g_{22}$  in [26]. (B)  $v = 0.235$  is supercritical for *both* components. This results in the formation of a dipole state which contains a vortex-lump pair, coupled to a lump-vortex pair, in a form similar to the stationary states reported in [13].

The last case (supersonic in both components) is examined in further detail in Fig. 4 for different velocities and widths of the quasi-1D obstacle. In the figure, the actual spatio-temporal evolution of the vorticity is shown. This clearly reveals the presence of a *vortex dipole* between the two components; moreover, this robust type of state appears to be clearly rotating, as time evolves. Furthermore, it can be noted that the wider the obstacle, the more complex the ensuing vortex patterns will be, with multiple vortex pairs being emitted.

*Conclusions.* We have considered the nucleation of coherent structures by a moving obstacle in two miscible BEC components. In one spatial dimension, we identified three different regimes: one without nucleation; one involving the nucleation of dark-antidark solitons previously predicted in stationary form in [24]; and one producing dark-dark soliton pairs, as well as dark-antidark dipoles. The critical points between these regimes were numerically obtained and, consistently with the corresponding single-component theory, were shown to approach the Landau criterion for impurity strength tending to zero; they were systematically lower than that as this strength increased. It was shown that similar behav-

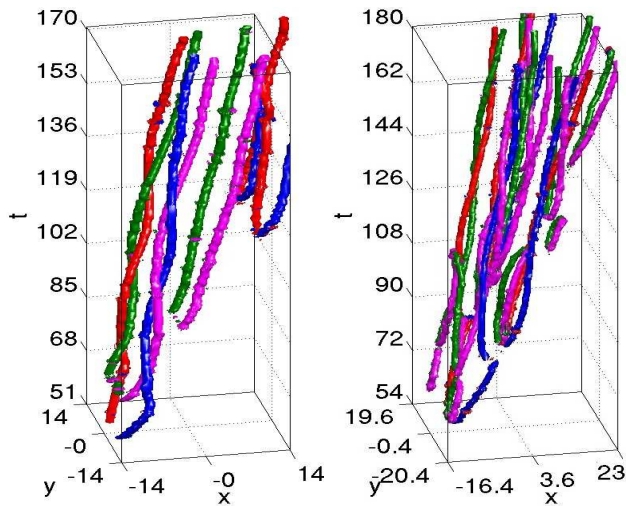


FIG. 4: (Color online). Vortex nucleation by a running impurity. The panels depict 3D contour plots of the vorticity  $\omega(x, y, t)$  for the different velocities and impurity size combinations: left panel:  $w = 15$  and  $v = 0.35$  and right panel:  $w = 20$  and  $v = 0.325$ . Both cases correspond to impurity velocities that are supersonic for *both* components. The red/blue isosurfaces correspond to positively/negatively charged vortices in the *first* component. We also superimpose the vorticity isocontours of the *second* component where green/magenta correspond to positive/negative vorticity. Note how *rotating vortex dipole* pairs between the two components are formed (left-most red-green and blue-magenta intertwined vorticity lines).

ior also occurs in the case of the harmonically trapped coupled BECs. We also examined the same type of behavior in 2D systems. We observed the existence of similar types of regimes, as in the 1D case (subcritical in both, supercritical in one, and supercritical in both). The intermediate regime gave rise to vortex-lump type structures (also discussed in [26]), while the supercritical regime gave the first example of nucleation of vortex-lump dipoles (obtained in stationary form in [13]), which were actually observed to be rotating as time evolved. This investigation indicates that there is an interesting spectrum of dynamical possibilities available in multi-component condensates, which it would certainly be relevant to explore experimentally. The recent realization of spinor condensates with more than two components may provide a fertile ground for further theoretical investigations in such higher-component settings.

*Acknowledgments.* PGK acknowledges support from NSF-DMS-0204585, NSF-DMS-0619492 and NSF-CAREER. RCG and PGK also acknowledge support from NSF-DMS-0505663. The work of BAM was partially supported by the Israel Science Foundation through the Center-of-Excellence grant No. 8006/03. Work at LANL is performed under the auspices of the US DoE.

- 
- [1] L.P. Pitaevskii and S. Stringari, *Bose-Einstein Condensation* (Oxford University Press, Oxford, 2003).
- [2] Yu.S. Kivshar and G.P. Agrawal, *Optical solitons: from fibers to photonic crystals* (Academic Press, San Diego, 2003).
- [3] M.J. Ablowitz, B. Prinari and A.D. Trubatch, *Discrete and Continuous Nonlinear Schrödinger Systems* (Cambridge University Press, Cambridge, 2004).
- [4] C. J. Myatt *et al.*, Phys. Rev. Lett. **78**, 586 (1997); D.S. Hall *et al.*, Phys. Rev. Lett. **81**, 1539 (1998).
- [5] D. M. Stamper-Kurn *et al.*, Phys. Rev. Lett. **80**, 2027 (1998).
- [6] G. Modugno *et al.*, Science **294**, 1320 (2001).
- [7] M. Mudrich *et al.*, Phys. Rev. Lett., **88**, 253001 (2002).
- [8] T.-L. Ho and V.B. Shenoy, Phys. Rev. Lett. **77**, 3276 (1996); H. Pu and N.P. Bigelow, Phys. Rev. Lett. **80**, 1130 (1998); B.D. Esry *et al.*, Phys. Rev. Lett. **78**, 3594 (1997).
- [9] Th. Busch *et al.*, Phys. Rev. A **56**, 2978 (1997); R. Graham and D. Walls, Phys. Rev. A **57**, 484 (1998); H. Pu and N.P. Bigelow, Phys. Rev. Lett. **80**, 1134 (1998); B.D. Esry and C.H. Greene, Phys. Rev. A **57**, 1265 (1998).
- [10] M. Trippenbach *et al.*, J. Phys. B **33**, 4017 (2000); S. Coen and M. Haelterman, Phys. Rev. Lett. **87**, 140401 (2001); B. A. Malomed *et al.*, Phys. Rev. A **70**, 043616 (2004).
- [11] P. Öhberg and L. Santos, Phys. Rev. Lett. **86**, 2918 (2001); Th. Busch and J.R. Anglin, Phys. Rev. Lett. **87**, 010401 (2001).
- [12] B. Deconinck *et al.*, J. Phys. A **36**, 531 (2003).
- [13] K. Kasamatsu *et al.*, Phys. Rev. Lett. **93**, 250406 (2004).
- [14] N.G. Berloff, Phys. Rev. Lett. **94**, 120401 (2005).
- [15] E.J. Mueller and T.-L. Ho, Phys. Rev. Lett. **88**, 180403 (2002); K. Kasamatsu, M. Tsubota and M. Ueda, Phys. Rev. Lett. **91**, 150406 (2003).
- [16] V. Hakim, Phys. Rev. E **55**, 2835 (1997).
- [17] A. Radouani, Phys. Rev. A **70**, 013602 (2004).
- [18] T. Frisch, Y. Pomeau and S. Rica, Phys. Rev. Lett. **69**, 1644 (1992); B. Jackson, J.F. McCann and C.S. Adams, Phys. Rev. Lett. **80**, 3903 (1998); T. Winiecki, J.F. McCann and C.S. Adams, Phys. Rev. Lett. **82**, 5186 (1999).
- [19] I. Carusotto *et al.*, cond-mat/0612114.
- [20] G.A. El *et al.*, Phys. Rev. Lett. **97**, 180405 (2006).
- [21] N. Pavloff, Phys. Rev. A **66**, 013610 (2002).
- [22] C. Raman *et al.*, Phys. Rev. Lett. **83**, 2502 (1999); R. Onofrio *et al.*, Phys. Rev. Lett. **85**, 2228 (2000).
- [23] C. Luo *et al.*, Science **299**, 368 (2003).
- [24] P.G. Kevrekidis *et al.*, Eur. Phys. J. D **28**, 181 (2004).
- [25] S. Inouye *et al.*, Nature **392**, 151 (1998); J.L. Roberts *et al.*, Phys. Rev. Lett. **81**, 5109 (1998).
- [26] N.G. Berloff, cond-mat/0412743.